2D+T METHOD DEVELOPMENT BASED ON EXTENDED VON KARMAN'S MOMENTUM THEORY: APPLICATION TO FREE-FALLING WATER ENTRY

Y. Lu*[1], A. Del Buono[2], T. Xiao[1], A. Iafrati[2] and J. Chen[1]
[1]College of Aerospace Engineering, Nanjing University of Aeronautics and Astronautics
Yudao Street 29 210016 Nanjing, People's Republic of China
[2]CNR-INM, INstitute of Marine engineering
Via di Vallerano 129 00128 Rome, Italy
*loux27@nuaa.edu.cn, alessandro.delbuono@inm.cnr.it, xthang@nuaa.edu.cn,
alessandro.iafrati@cnr.it, chenjch@nuaa.edu.cn

ABSTRACT: The present study propose a theoretical prediction method of the fluid force acting on a free-falling body, introducing a developed 2D+t method, where the body is cut into a series of slices. The hydrodynamic behaviors of each slice are obtained by the extended von Karman's momentum theory. This capability of the proposed method could be seen as a promising tool for theoretically predicting hydrodynamic behaviors during aircraft ditching.

1. INTRODUCTION

Aircraft ditching is one of the most extreme emergency circumstances that involves the intentional impact of an aircraft with water and includes four phases such as approach, impact, landing and floatation [1]. In a planned ditching event predicting hydrodynamic loads is very important to guarantee safety and ensure the certifications' respect. To address related problems about the hydrodynamic behaviors, researchers have developed theoretical methods using a series of mathematical models [2, 3], conducted scaled-model experimental tests in the water tanks [4, 5], and employed numerical strategies with various discretization ideas, such as the finite volume method [6], finite element method [7, 8], smoothed particle hydrodynamics method [9, 10] and lattice Boltzmann with immersed boundary method [11]. These efforts have been steadily advancing. After carefully evaluating the advantages and disadvantages in the concept and preliminary design process, the latter two are deemed to be time-consuming and expensive, whereas the former is more commonly favored due to its high efficiency.

The same is for planing craft in calm water where predicting the vertical force is quite important [12]. Besides high-fidelity approaches, the use of fast and efficient solvers, albeit of lower fidelity, is of primary interest for evaluating hydrodynamics loads in this kind of events. In this perspective the 2D+t method can be considered as a valid option with its high calculation efficiency. The 2D+t method is based on a slender body approximation and transforms the three dimensional hydrodynamic problem into a series of two-dimension cross-section water-entry problems ignoring the axial flow effect, with the shape and displacement of the section changing in time, in an earth-fixed frame of reference. Thus, it is clear how the reliability of the 2D+t method depends heavily on the accuracy and efficiency of the 2D solver used.

By looking at the aircraft ditching problem from a 2D+t perspective, the type of motion for each section can be treated either as a case of prescribed motion or as a case of free fall. The present paper proposes a 2D+t multisection procedure to solve the hydrodynamic force of a 3D free-fall model, similar to aircraft ditching case, that exploits the extended von Karman's momentum theory developed for the water impacting of a free-falling symmetric wedge [13].

Therefore, the present work outlines as follows. Section 2. presents the methodology for the theoretical and numerical approaches, together with the detailed validation model and

computational setup, the main results are reported and discussed in Sec. 3. and final conclusions are drawn in Sec. 4. .

2. METHODOLOGY AND NUMERICAL PROCEDURE

2.1 Development of 2D+t method

Pioneer research in water-entry problem has been conducted by von Karman [14], based on momentum theorem and the added mass for the force prediction as the wedge-shaped body penetrates the water surface. The theorem of momentum equation, used to predict the hydrodynamic load during water entry impact, is expressed as follows:

$$M\upsilon_{z0} = (M + m_{\text{added}}) \cdot \upsilon_z(t) \tag{1}$$

where M is the mass of the wedge per meter, υ_{z0} is the initial vertical velocity before the impact, $\upsilon_z(t)$ is the instantaneous velocity during impacting and m_{added}, namely added mass briefly computed by $m_{\text{added}} = (\pi\rho r^2(t))/2$ (see Fig. 1), using the flat-plate approximation of the added mass. It is assumed the a half disk of water with radius $r(t)$ is moving together with the wedge, ignoring the effect of water pile-up herein.

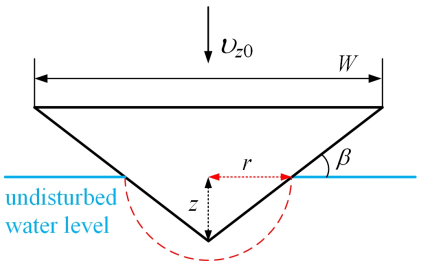

Figure 1 - Illustration of the water-entry scenario for the wedge.

Referring to the extended von Karman's momentum theory [13] for the wedge falling freely into water, it is possible to compute the maximal impact acceleration $a_{z\max}$ and the corresponding velocity υ_z^*, penetration depth z^* and time t^* when acceleration reaches its peak value:

$$a_{z\max} = \upsilon_{z0}^2 \left(\frac{5}{6}\right)^3 \frac{\gamma_D}{\tan(\beta)} \sqrt{\frac{2\pi\rho}{5M}} \tag{2a}$$

$$z^* = \sqrt{\frac{2M}{5\pi\rho\gamma_D^2}} \tan(\beta) \tag{2b}$$

$$\upsilon_z^* = \frac{5}{6}\upsilon_{z0} \tag{2c}$$

$$t^* = \frac{1}{\upsilon_{z0}} \frac{16}{15} \sqrt{\frac{2M}{5\pi\rho\gamma_D^2}} \tan(\beta) \tag{2d}$$

where γ_D is the pile-up coefficient derived from Dobrovol'skaya's solution [15, 16]. It is proved to be dependent on the deadrise angle β, defined as $\gamma_D = -0.0114\beta + 1.5669$. As highlighted in the previous study, it is evident that the values of $a_{z\max}$, υ_z^*, z^* and t^* are primarily influenced by three key parameters (β, M and υ_{z0}). Building on this observation, the scaled parameters $\tilde{a}_z$,

$\tilde{\upsilon}_z$, $\tilde{z}$ and $\tilde{t}$ are then expressed as:

$$\tilde{a}_z = a_z(t) \cdot \frac{\sqrt{M}}{\upsilon_{z0}^2} \cdot \frac{\tan(\beta)}{\gamma_D} \tag{3a}$$

$$\tilde{\upsilon}_z = \frac{\upsilon_z(t)}{\upsilon_{z0}} \tag{3b}$$

$$\tilde{z} = z(t) \cdot \frac{1}{\sqrt{M}} \cdot \frac{\gamma_D}{\tan(\beta)} \tag{3c}$$

$$\tilde{t} = t \cdot \frac{\upsilon_{z0}}{\sqrt{M}} \cdot \frac{\gamma_D}{\tan(\beta)} \tag{3d}$$

Furthermore, the quantitative relationships described by Eq. (3) are applicable not only for the peak acceleration but also throughout the impacting phase, encompassing the correlated parameters. Thus, characteristic curves ($\tilde{\upsilon}_z$-$\tilde{z}$ and $\tilde{a}_z - \tilde{z}$) can be obtained during a free-fall water entry of a wedge with a wide range of υ_{z0}, β and M when the instantaneous Froude number Fr^* is greater than 6.5 [13]. It is worth noting that the characteristic curves serve two distinct implications:

a) a unified pattern derived from various cases.

b) each point on the characteristic curve corresponds to different conditions using varying scaling factors (β, M and υ_{z0}).

Let now consider, as an example, the vertical free-fall water entry of a wedge-shaped prismatic, as depicted in Fig. 2. At the time instant $t = t_i$, the instantaneous penetration velocity $\upsilon_z(t_i)$ and depth z of the body are first determined. By applying the 2D+t method, the body can be split into multiple slices. i.e. the two arbitrary slices denoted as m^{th} and n^{th}, which have the same velocity $\upsilon_z(t_i)$, mass M and dearise angle β, but different penetration depths, z^m and z^n respectively, which can be easily obtained from geometric calculations on the body.

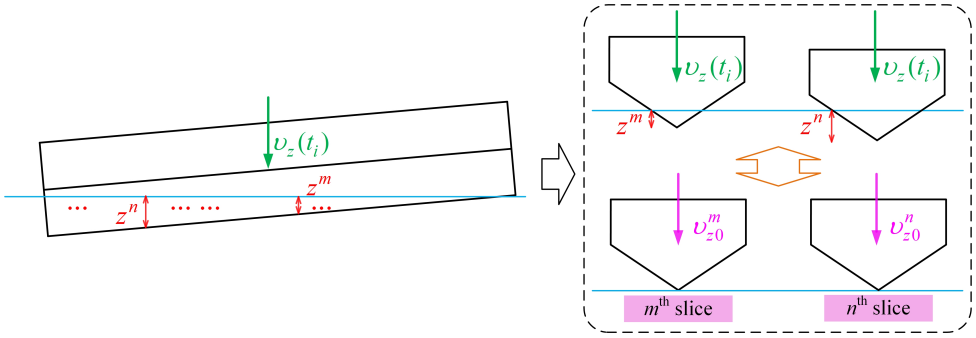

Figure 2 - Explanation of the developed 2D+t method applied to the water-entry scenario of a wedge-shaped prismatic body with multiple slices.

To figure out the total hydrodynamic force exerting on the body, the fundamental idea is that, the hydrodynamic force on these two slices (penetration depth at z^m and z^n) can be treated in relation to free-fall water entry cases with different initial vertical velocities υ_{z0}^m and υ_{z0}^n. This implies that multiple slices derived from the prismatic body simultaneously can be interpreted as distinct free-fall water entry cases of 2D wedge-shape with different initial vertical velocities. Note that the effect of fluid flow along the longitudinal direction is not considered herein.

A crucial aspect of this approach is the use of the known parameters ($\upsilon_z(t_i)$ and z^j) and characteristic curves, derived from the extended von Karman's momentum theory [13], to infer the corresponding hydrodynamic force for the j^{th} slice. Note that the variable j represents the number of the slice ($j = 1, \cdots, m, \cdots, n, \cdots$). In previous study [13], it has been demonstrated

the way from the relationship between the instantaneous velocity $\upsilon_z$and the penetration depth z for different conditions (β, M and υ_{z0}) to obtaining the characteristic curve related to $\tilde{\upsilon}_z - \tilde{z}$ after removing the variable parameters (see the first column in Fig. 3).

As the characteristic curve ($\tilde{\upsilon}_z - \tilde{z}$) serves as a unified scaling law for all free-fall water entry cases [13], in the 2D+t perspective, all parameters are already known, except for the value of υ_{z0}^j. The latter can be derived from the characteristic curve associated with several parameters ($\upsilon_z(t_i)$, z^j, $\tilde{\upsilon}_z^j$ and $\tilde{z}^j$), $\upsilon_{z0}^j = \upsilon_z(t_i)/\tilde{\upsilon}_z^j$, as shown in the second column in Fig. 3. By this way, this derivation process, further points out the corresponding free-fall water entry case with the initial velocity υ_{z0}^j when the j^{th} slice enters into water with penetration depth z^j and velocity $\upsilon_z(t_i)$, as shown in Fig. 2.

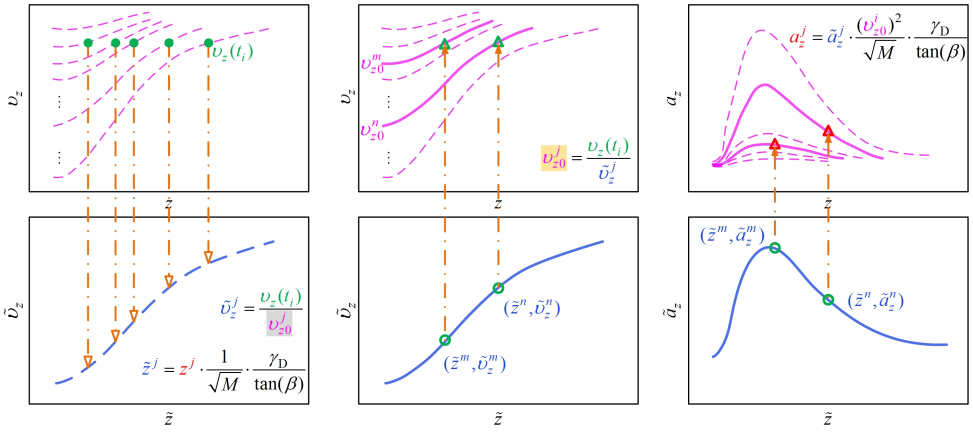

Figure 3 - Inversion process of characteristic curves for free-fall water entry.

Similarly, the acceleration of the j^{th} slice can be determined using the characteristic curve ($\tilde{a}_z - \tilde{z}$, see the third column in Fig. 3) together with the following formula:

$$a_z^j = \tilde{a}_z^j \cdot \frac{(\upsilon_{z0}^j)^2}{\sqrt{M}} \cdot \frac{\gamma_D}{\tan(\beta)} \tag{4}$$

where the value of $\tilde{a}_z^j$ is directly extracted from the characteristic curve with the help of $\tilde{z}^j$. Next, it is possible to evaluate the 2D hydrodynamic force acting on each j^{th} slice and, consequently, the total fluid force $\hat{F}_z$ exerting on the prismatic body can be derived from the sum of all slices' 2D hydrodynamic forces.

2.2 Validation case

The proposed 2D+t multisection approach has been validated for the case of vertical free-fall water entry of a varying cross-section prismatic body, as seen in Fig. 4. The prism has a width W=0.2 m, length L=0.35 m and mass m=1 kg (density ρ=486 kg/m^3), associated with a deadrise angle β ranging from 10° on one side to 45° on another side.

A comparison with the CFD results computed by using the commercial package Star CCM+ as the two-phase flow solver has been done for validation. In the present study the unsteady incompressible Reynolds-averaged Navier-Stokes equations, coupled with a standard $k-\omega$ two-equation turbulence model, are solved using the finite volume method and the Volume of Fluid (VOF) scheme, to capture the water-air interface.

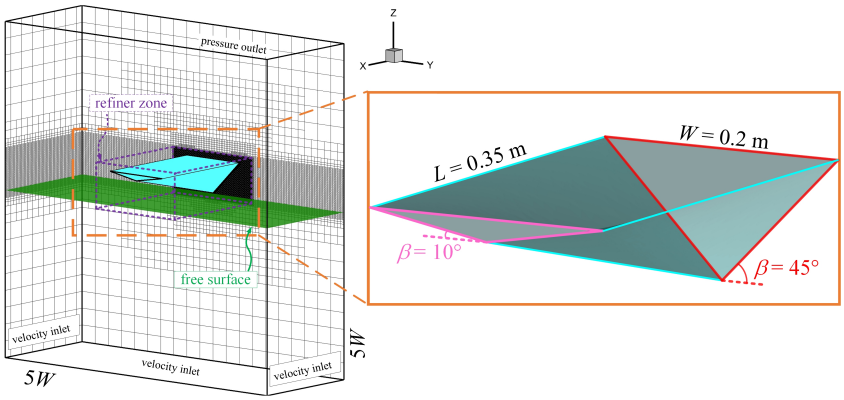

Figure 4 - Schematic representation of the prismatic body with varying cross-section and the computational domain.

3. RESULTS AND DISCUSSION

For further explaining the operation process of the proposed 2D+t method, the case of the varying cross-section prismatic body entering water freely with initial vertical velocity υ_{z0}=4 m/s is investigated in the present study. Fig. 5 shows the time histories of kinematic parameters for the prism, such as acceleration a_z, instantaneous penetration velocity υ_z and instantaneous penetration depth z. Note that positive values of these three parameters are in the opposite direction of gravity. The time instant t=0.01 s is selected as a test point, as shown in Fig. 5. The detailed kinematic information for this moment is collected in Table. 1.

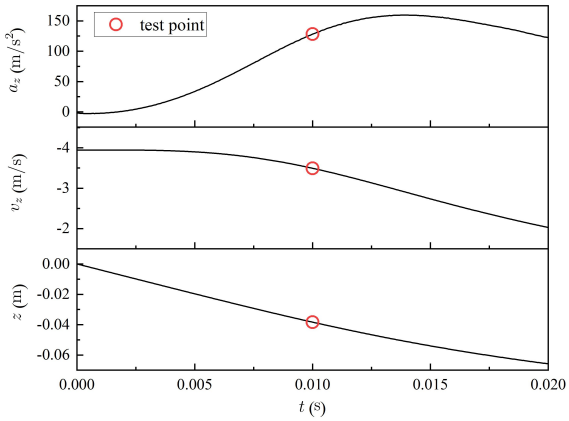

Figure 5 - Time histories of kinematic parameters for the varying cross-section prismatic body during free-fall water entry.

Table 1 - Detailed kinematic information of the prism at t=0.01s.

t, s	$\upsilon_z(t_{0.01})$, m/s	a_z, m/s^2	$z(t_{0.01})$, m	ΔZ, m	ΔL, m
0.01	-3.4943	128.1588	-0.0383	0.0383	0.1627

Concerning the characteristic curves in the present study, data are derived from a simulated wedge case with a specific set of parameters ($\beta = 45°$, M=4.6842 kg/m and υ_{z0}=5.5 m/s [13]), as shown in Fig. 6. It is worth noting that there is only one general standard for the chosen

parameters, that is the instantaneous Froude number $Fr^* > 6.5$, as mentioned in the work of Lu et al [13]. Subsequently, the characteristic curves are fitted with polynomial formula, as presented in Eqs. (5) and (6).

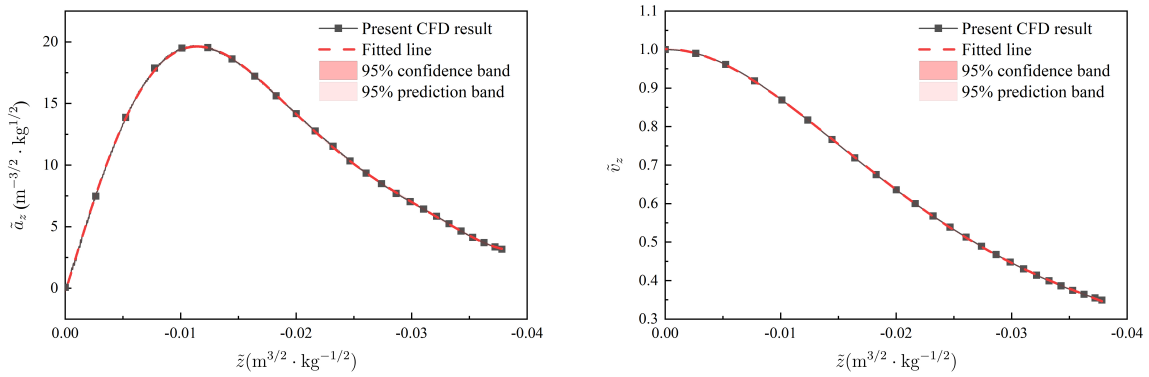

Figure 6 - Characteristic curves for wedge free-fall water entry: a) $\tilde{a}_z$ versus $\tilde{z}$; b) $\tilde{v}_z$ versus $\tilde{z}$.

$$\tilde{a}_z = -0.35026 - 3093.66877\tilde{z} + 11743.57797\tilde{z}^2 + 2.26181E7\tilde{z}^3 + 1.28322E9\tilde{z}^4 + 2.8479E10\tilde{z}^5 + 2.29482E11\tilde{z}^6 \tag{5}$$

$$\tilde{v}_z = 1.00131 - 0.36998\tilde{z} - 1852.65292\tilde{z}^2 - 56703.97435\tilde{z}^3 - 531047.33189\tilde{z}^4 \tag{6}$$

Next, the discretization strategy has to be considered on the characteristic curves. Fig. 7 shows the schematic diagram of slices on the prismatic body when t=0.01 s, where the submerged part of the body is cut into several slices equally. The thickness d and penetration depth z^j of the j^{th} slice are defined as:

$$d = \frac{\Delta L}{n} \tag{7}$$

$$z^j = \frac{(1-2j)\cdot\Delta Z}{2n} \tag{8}$$

where n represents the chosen number of slice on the body. Note that the value of z^j is negative.

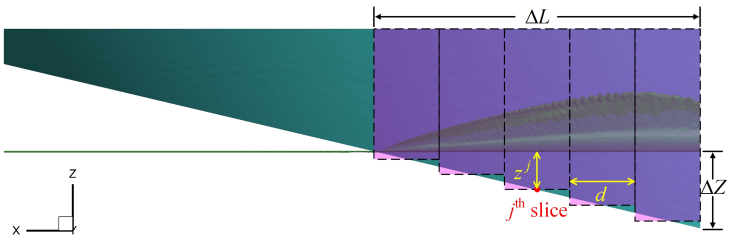

Figure 7 - Schematic diagram of slices on the prismatic body at t=0.01s.

Due to the different cross sections along the longitudinal axis of the body, each slice has different value of mass M^j and deadrise angle β^j. Thus, the characteristic penetration depth $\tilde{z}^j$ of the j^{th} slice, referring to Eq. (3c), has to be modified as:

$$\tilde{z}^j = z^j \cdot \frac{1}{\sqrt{M^j}} \cdot \frac{\gamma_D}{\tan(\beta^j)} \tag{9}$$

and the expressions of M^j and β^j are:

$$M^j = \frac{W}{2} \cdot \left(\frac{W}{2} - \Delta Z - z^j\right) \cdot \rho \tag{10}$$

$$\beta^j = \arctan\left[\frac{2}{W} \cdot \left(\frac{W}{2} - \Delta Z - z^j\right)\right] \tag{11}$$

Then, the characteristic velocity $\tilde{\upsilon}_z^j$ and characteristic acceleration $\tilde{a}_z^j$ of the j^{th} slice are easily obtained through Eqs. (5) and (6), as well as the corresponding initial velocity for the j^{th} slice, $\upsilon_{z0}^j = \upsilon_z(t_{0.01})/\tilde{\upsilon}_z^j$. Finally, the total fluid force $\hat{F}_z$ exerted on the prismatic body can be obtained using the proposed 2D+t method as follows:

$$\begin{aligned}\hat{F}_z &= \sum_{j=1}^{n} \hat{F}_z^j \\ &= \sum_{j=1}^{n} \left[M^j \cdot (a_z^j + g) \cdot d\right] \\ &= \sum_{j=1}^{n} \left\{M^j \cdot \left[\tilde{a}_z^j \cdot \frac{(\upsilon_{z0}^j)^2}{\sqrt{M^j}} \cdot \frac{\gamma_D}{\tan(\beta^j)} + g\right] \cdot d\right\}\end{aligned} \tag{12}$$

Furthermore, the convergence of the solution on fluid force is also investigated when increasing the number of slices. As it can be observed in Fig. 8, the theoretical results approach a constant value as the number of slices increases. Referring to the grid convergence index (GCI) method for assessing uncertainty in the CFD simulation, present theoretical uncertainty arising from discretization errors in predicting fluid forces is considered. Based on this study the Richardon extrapolated value of fluid force on prism at t=0.01s is estimated to be 147.7947 N with an error band of 0.0205% (see the red diamond symbol in Fig. 8). A good agreement with the present CFD result (137.9688 N) is obtained with a small difference 7.12%. Besides, Fig. 9 shows the comparison of extrapolated fluid forces derived from the proposed 2D+t method and the present CFD results over time, indicating that the present theoretical estimate agrees well with the CFD result with a minor deviation being below 10% in the whole process of free-fall water entry.

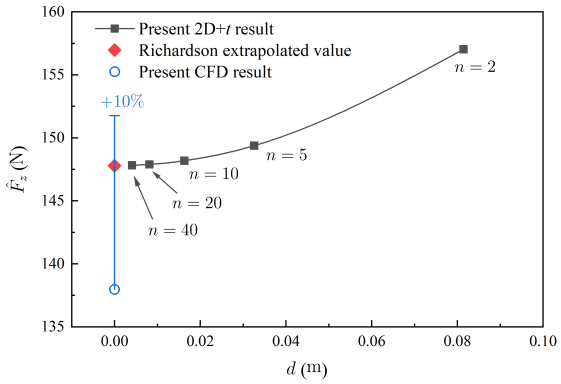

Figure 8 - Fluid force obtained from the proposed 2D+t method with different thickness d compared with the present CFD result at t=0.01s.

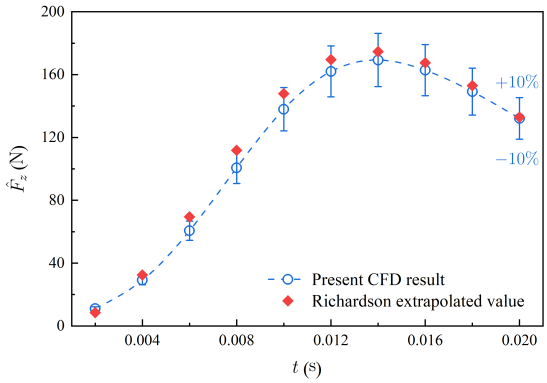

Figure 9 - Comparison of extrapolated fluid forces derived from the proposed 2D+t method and the present CFD results during prismatic body water-entry scenario.

4. CONCLUSION

The present study focuses on the theoretical prediction of the fluid force acting on a free-falling body, introducing a developed 2D+t method, in which the body is cut into a series of slices. The hydrodynamic behaviors of each slice are obtained by the extended von Karman's momentum theory. The main contributions and findings are summarized as follows:

(1) The methodological approach, from constructing characteristic curves to clarifying kinematic parameters and the discretization and sum process, provides a clear pathway for the proposed 2D+t method.

(2) Characteristic curves, derived from the extended von Karman's momentum theory, are employed to compute the fluid force acting on each individual slice. which has various combination of variables, such as penetration velocity and the inherent parameter deadrise angle and mass.

(3) A detailed analysis of the proposed 2D+t method is undertaken using a case study of a varying cross-section prismatic body in free fall. Comparing the results of present 2D+t method and present CFD method at diverse temporal instants during free fall, a high level of agreement is achieved with minor deviation less than 10%. It is expected to be extended to address the unsteady motion of bodies subjected to gravity force, especially for multiple degrees of freedom. This capability positions the proposed 2D+t method as a promising tool for theoretically predicting hydrodynamic behaviors during aircraft ditching.

ACKNOWLEDGMENTS

This work has been supported by the Aeronautical Science Foundation of China (No. 20220023052001 and No. 20230023052001).

5. REFERENCES

1. Hughes, K., Vignjevic, R., Campbell, J., Vuyst, T. D., Djordjevic, N. and Papagiannis, L. (2013) From aerospace to offshore: bridging the numerical simulation gaps-simulation advancements for fluid structure interaction problems. *Int. J. Impact Eng.* 61, 48-63

2. Kanyoo, P. (2016) Mathematical model of high speed planing dynamics and application to aircraft ditching. *University of Southampton*, Southampton

3. Del Buono, A., Bernardini, G. and Iafrati, A. (2021) Multisection approach for the vertical water impact of a fuselage. *AIDAA XXVI International Congress*, Pisa, 1-6

4. Iafrati, A., Grizzi, S. and Olivieri, F. (2021) Experimental investigation of fluid-structure interaction phenomena during aircraft ditching. *AIAA J.* 59(5), 1561-1574

5. Spinosa, E., Broglia, R. and Iafrati, A. (2022) Hydrodynamic analysis of the water landing phase of aircraft fuselages at constant speed and fixed attitude. *Aerosp. Sci. Technol.* 130, 107846

6. Qu, Q., Liu, C., Liu, P., Guo, B. and Agarwal, R. K. (2016) Numerical simulation of water-landing performance of a regional aircraft. *J. Aircraft* 53(6), 1680-1689

7. Siemann, M. H., Schwinn, D. B., Scherer, J. and Kohlgruber, D. (2017) Advances in numerical ditching simulation of flexible aircraft models. *Int. J. Crashworthiness* 23(2), 236-251

8. Siemann, M. N. and Langrand, B. (2017) Coupled fluid-structure computational methods for aircraft ditching simulation: comparison of ALE-FE and SPH-FE approaches. *Comput. Struct.* 188, 95-108

9. Xiao, T., Qin, N., Lu, Z., Sun, X., Tong, M. and Wang, Z. (2017) Development of a smoothed particle hydrodynamics method and its application to aircraft ditching simulations. *Aerosp. Sci. Technol.* 166, 28-43

10. Xiao, T., Lu, Z. and Deng, S. (2021) Effect of initial pitching angle on helicopter ditching characteristics using SPH method. *J. Aircraft* 58(1), 167-181

11. Wu, Z. and Guo, L. (2023) A new approach to aircraft ditching analysis by coupling free surface lattice boltzmann and immersed boundary method incorporating surface tension effects. *Ocean Eng.* 286, 115559

12. Shao, W., Ma, S., Duan, W., Liu, J. and Zhang, Y. (2023) Vertical force prediction of planing craft in calm water based on variable section slamming model. *Ocean Eng.* 287, 115693

13. Lu, Y., Del Buono, A., Xiao, T., Iafrati, A., Xu, J., Deng, S. and Chen, J. (2023) Parametric study on the water impacting of a free-falling symmetric wedge based on the extended von Karman's momentum theory. *Ocean Eng.* 271, 113773

14. von Karman, T. (1929) The impact on seaplane floats during landing. *NACA*, Washington, D. C., 1-10

15. Dobrovol'skaya, Z. N. (1969) On some problems of similarity flow of fluids with a free surface. *J. Fluid Mech.* 36(4), 805-829

16. Zhao, R. and Faltinsen, O. M. (1993) Water entry of two-dimensional bodies. *J. Fluid Mech.* 246, 593-612